Supplementary Information

Enhanced Carrier Mobility-Driven Performance Improvement in Colloidal Quantum Dot Solar Cells

Yongwoo Jeon[a,b▽], Hong Gu Kang[c▽], Seohee Park[a,b▽], Younghyun Kim[d], Seong-Yong Cho[c,d], Dennis T. Lee[e], Younghoon Kim[f], Byeong Guk Jeong[g]*, Sohee Jeong[b]*, Jung Hoon Song[h]*, Ju Young Woo[a,c,i]*

[a] Department of Autonomous Manufacturing & Process R&D, Korea Institute of Industrial Technology (KITECH), Ansan 15588, Republic of Korea

[b] Department of Energy Science (DOES), Center for Artificial Atoms, Institute of Energy Science and Technology (SIEST), Sungkyunkwan University (SKKU), Suwon 16419, Republic of Korea

[c] HYU-KITECH Joint Department, Hanyang University, Ansan 15588, Republic of Korea

[d] Department of Photonics and Nanoelectronics, Hanyang University, Ansan 15588, Korea

[e] Department of Materials Science and Chemical Engineering, Stony Brook University, Stony Brook, NY 11790, USA

[f] Department of Chemistry, Kookmin University, Seoul 02707, Republic of Korea

[g] Institute for Environment and Energy, School of Chemical Engineering, Pusan National University, Busan 46241, Republic of Korea

[h] Department of Semiconductor Engineering, Semiconductor Nanotechnology Research Institute, Mokpo National University, Muan 58554, Republic of Korea

[i] School of Integrative Engineering, Chung-Ang University, Seoul 06974, Republic of Korea

▽ These authors contributed equally to this work.

*e-mail: jywoo@kitech.re.kr (Dr. Ju Young Woo)

*e-mail: jhsong@mnu.ac.kr (Prof. Jung Hoon Song)

*e-mail: s.jeong@skku.edu (Prof. Sohee Jeong)

*e-mail: bgjeong@pusan.ac.kr (Prof. Byeong Guk Jeong)

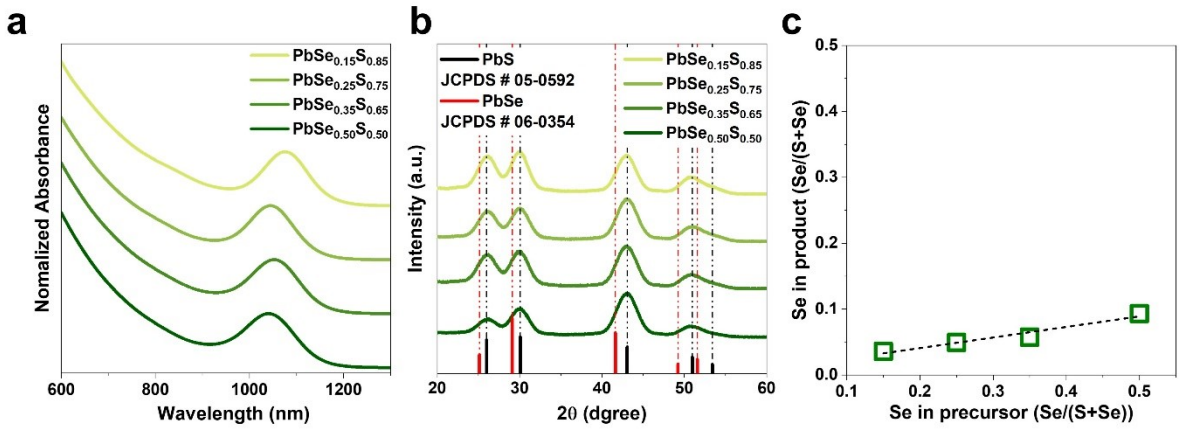

Figure S 1. (a) Absorption spectra, (b) XRD patterns, and (c) actual Se composition determined by ICP analysis of ternary PbSSe quantum dots synthesized without a highly reactive Se precursor, as a function of anion ratio.

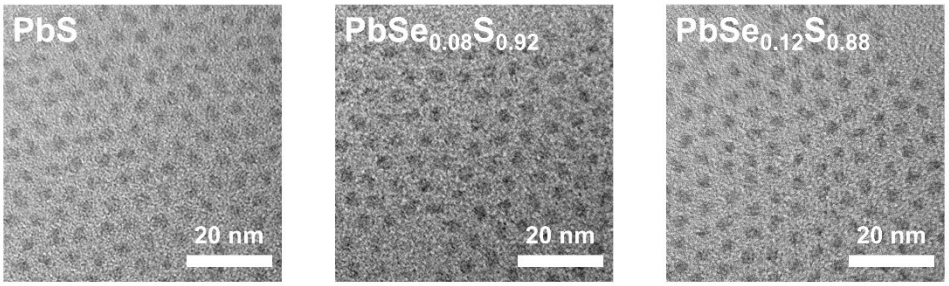

Figure S 2. TEM images of PbS quantum dots and ternary PbSSe quantum dots synthesized with the addition of a highly reactive Se precursor.

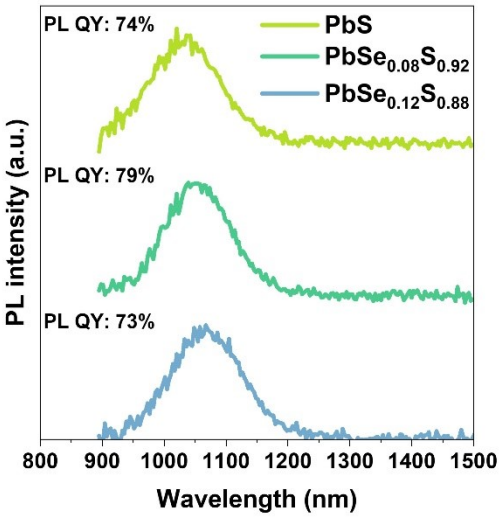

Figure S 3. Photoluminescence quantum yield (PL QY) comparison between binary PbS quantum dots and ternary PbSeS quantum dots.

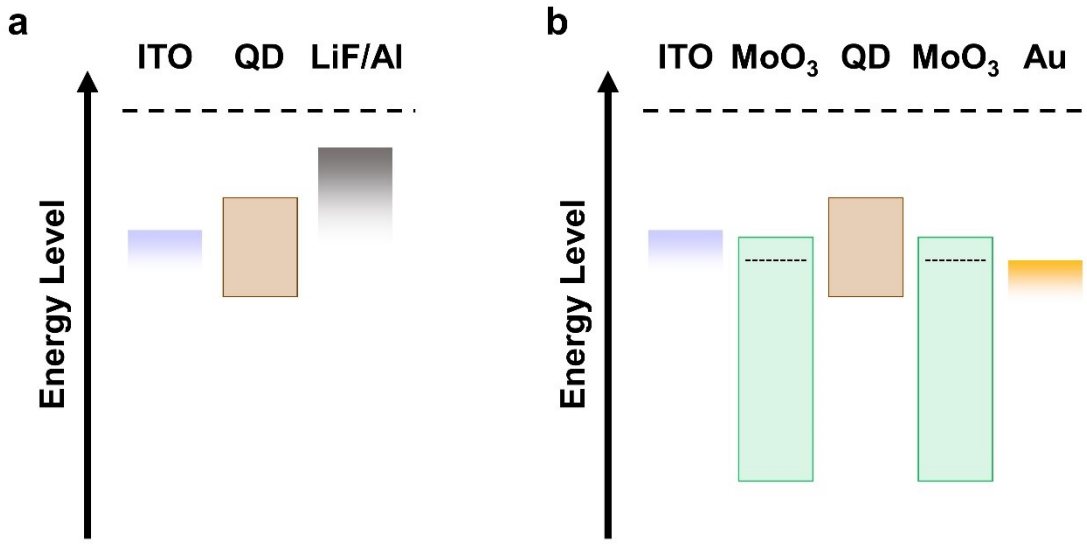

Figure S 4. Energy band diagrams for SCLC measurements: (a) electron-only device (EOD) and (b) hole-only device (HOD).

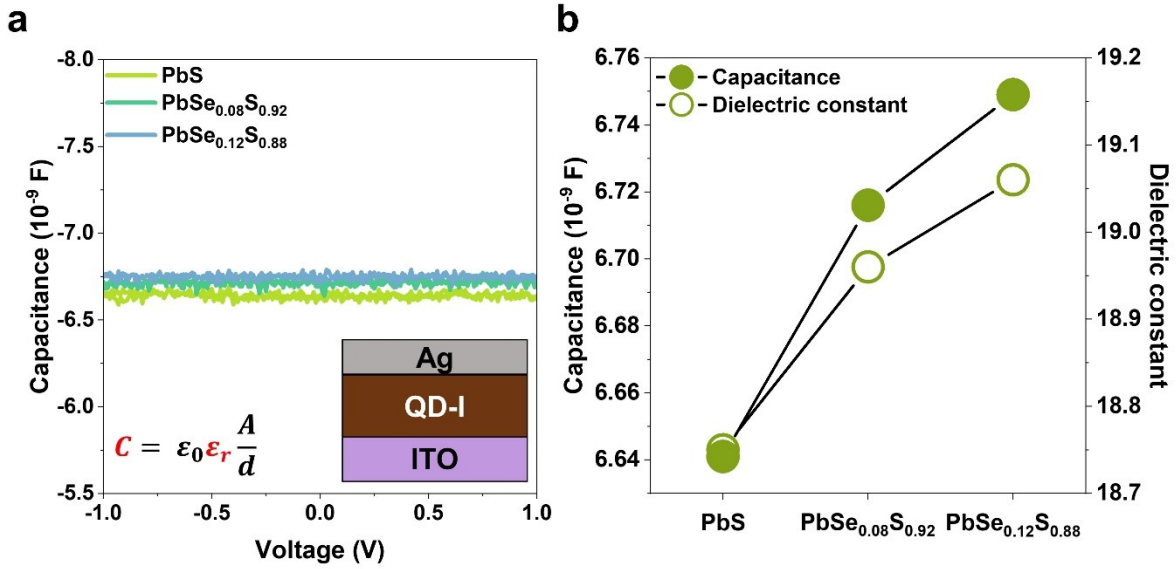

Figure S 5. (a) Capacitance as a function of voltage sweep for different anion compositions, and (b) dielectric constants calculated from the measured capacitance values.

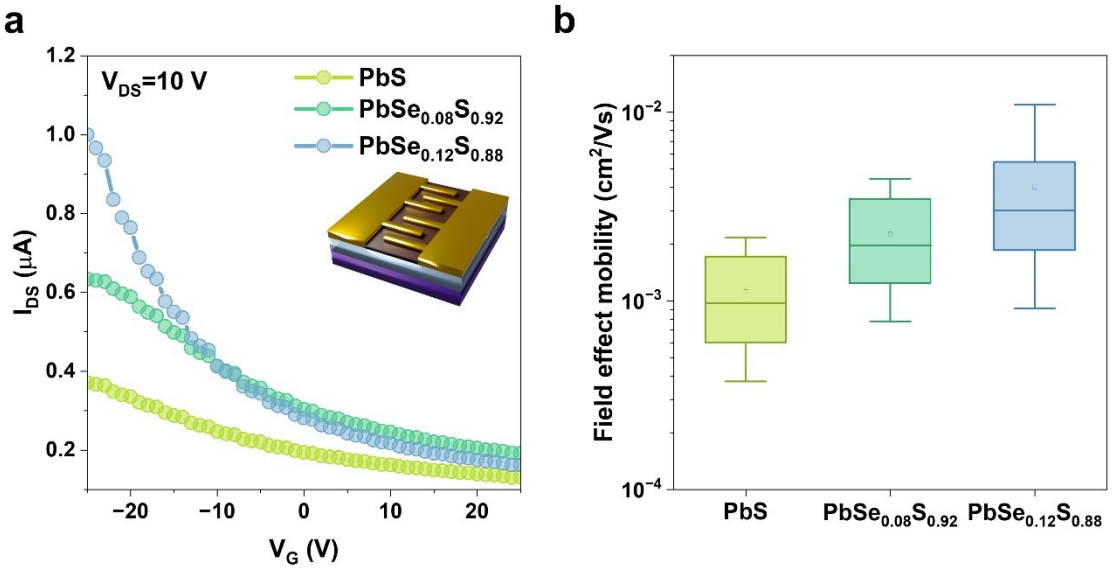

Figure S 6. (a) Transfer curves of FETs based on PbS and ternary PbSeS quantum dots. (channel length: 5 μm; width: 300 μm) (b) Field-effect mobility of majority carrier (hole) extracted in the linear regime.

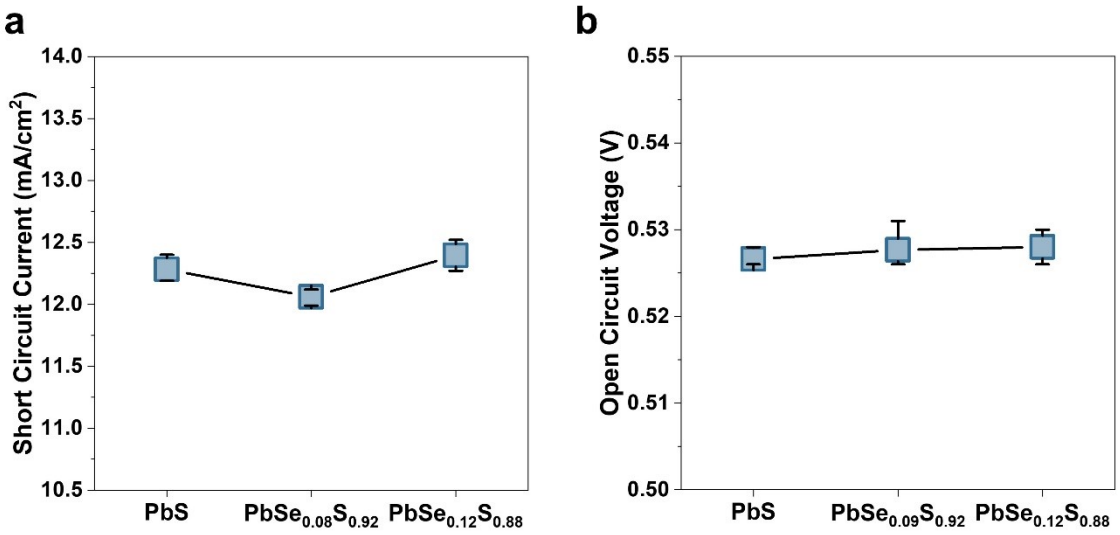

Figure S 7. (a) Short-circuit current density (J_{SC}) and (b) open-circuit voltage (V_{OC}) of fully depleted devices with identical active layer thickness, as a function of Se composition.

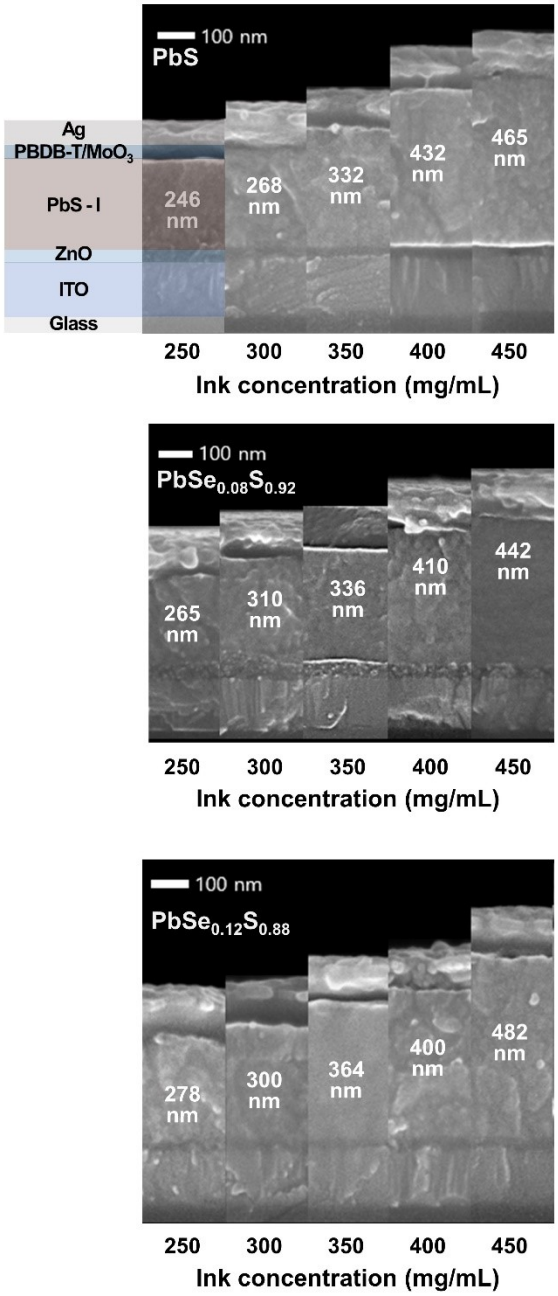

Figure S 8. Cross-sectional SEM images of devices fabricated with varying ink concentrations for each anion composition.

PbS	246 nm	268 nm	332 nm	432 nm	465 nm
Short circuit current (mA/cm²)	23.79	23.64	24.85	25.83	23.60
Open circuit voltage (V)	0.556	0.550	0.550	0.554	0.539
Fill factor (%)	56.67	53.64	54.05	51.82	45.75
Power conversion efficiency (%)	7.50	6.97	7.40	7.41	5.82

$PbSe_{0.08}S_{0.92}$	265 nm	310 nm	336 nm	410 nm	442 nm
Short circuit current (mA/cm²)	24.68	23.89	25.11	27.23	26.70
Open circuit voltage (V)	0.558	0.551	0.549	0.554	0.551
Fill factor (%)	58.75	56.86	55.58	53.95	51.79
Power conversion efficiency (%)	8.08	7.48	7.66	8.14	7.63

$PbSe_{0.12}S_{0.88}$	278 nm	300 nm	364 nm	400 nm	482 nm	559 nm
Short circuit current (mA/cm²)	25.01	24.94	26.21	28.04	28.25	27.70
Open circuit voltage (V)	0.550	0.550	0.548	0.549	0.546	0.545
Fill factor (%)	59.48	58.33	56.42	55.50	55.64	54.78
Power conversion efficiency (%)	8.17	8.00	8.10	8.54	8.59	8.27

Table S 1. Summary of solar cell performance for devices with different anionic compositions and varied active layer thicknesses. The thickness values were estimated from cross-sectional SEM images.